Bull. Mater. Sci. (2020) 43:27
https://doi.org/10.1007/s12034-019-1964-4

A kaolinite/TiO_2/ZnO-based novel ternary composite for photocatalytic degradation of anionic azo dyes

A K M MAKSUDUL HASAN[1], SHAIKAT CHANDRA DEY[1], MUHAMMAD MOMINUR RAHMAN[2], ABDULLAH MUHAMMAD ZAKARIA[3], MITHUN SARKER[1,4], MD ASHADUZZAMAN[1] and SAYED MD SHAMSUDDIN[1,*]

[1]Department of Applied Chemistry and Chemical Engineering, Faculty of Engineering and Technology, University of Dhaka, Dhaka 1000, Bangladesh

[2]Department of Chemistry, Virginia Tech, Blacksburg, VA 24061, USA

[3]Département de médecine Nucléaire et Radiobiologie, Faculté de médecine et des sciences de la santé, Université de Sherbrooke, Sherbrooke J1H 5N4, Canada

[4]Department of Chemistry and Green-Nano Materials Research Center, Kyungpook National University, Daegu 41566, Republic of Korea

*Author for correspondence (sdin@du.ac.bd)

MS received 30 January 2019; accepted 3 June 2019; published online 18 December 2019

Abstract. Solar-assisted photocatalytic degradation of organic pollutants has emerged as efficient technology for the effective treatment of industrial wastewater. Here, we report a simple technique for the fabrication of a novel ternary photocatalyst from kaolinite (K), TiO_2 (T) and ZnO (Z). The most efficient catalyst was prepared at a calcination temperature of 600°C. The fabricated ternary composite was characterized using different analytical techniques including Fourier transform infrared spectroscopy, X-ray diffraction, thermogravimetric analysis, scanning electron microscopy, field emission-scanning electron microscopy and energy dispersive X-ray spectroscopy. The photocatalytic degradation was performed at room temperature (25°C) using Remazol Red (RR), an anionic azo dye, as the model compound. A maximum of 98% degradation of RR was found with the ternary catalyst $K_{0.50}T_{0.45}Z_{0.05}$, which was prepared from 50% kaolinite (w/w), 45% TiO_2 (w/w) and 5% ZnO (w/w). The catalyst was found to be suitable for long-term repeated applications. Mechanistic investigation through radical trapping experiments confirmed hydroxyl radicals as the potential contributor to the photocatalytic degradation of RR. It is highly expected that a novel photocatalyst design such as this will pave way towards further development of materials capable of hazardous dye removal from industrial effluents.

Keywords. Solar-assisted; photocatalyst; kaolinite; calcination; Remazol Red.

1. Introduction

The release of wastewater from various industries is an emerging concern for environmentalists [1]. The effluents from textile industries carry significant quantities of unused dyes and direct disposal of these dyes into the nearby water bodies without any prior treatment causes severe water pollution [2,3]. Besides, the exposure to these recalcitrant dyes has severe consequences including fatal diseases like cancer, mutagenic changes, delayed nervous responses, neurological disorders, etc. [2,3]. Various expensive physical, chemical and biological methods have been traditionally applied to remove this type of pollutant from wastewater [4,5]. In most of the cases, these methods are highly time and energy consuming and non-economical [6]. Instead of complete degradation, the pollutants are rather simply transferred into other environmentally hazardous forms [7]. Chemical treatment methods suffer from using hazardous oxidants, while biodegradation is selective in nature [8]. In order to overcome these challenges, developing more efficient techniques of dye removal from wastewater has become a dire need. In this perspective, major attention has been paid to photocatalytic degradation of dyes, which is a rapidly emerging technology for wastewater purification. Using this efficient technology, nearly complete degradation of dyes is possible [9].

Recently, the degradation of various organic pollutants using semiconductor photocatalysts has been widely studied [10–12]. In the case of photocatalytic degradation, electron–hole pairs are generated by absorbing band-gap energy from an external source, which leads to effective redox reactions with species adsorbed on the surface of the photocatalysts [13]. Due to its several advantages such as high-photocatalytic activity, high-photochemical stability, inexpensive nature and non-toxicity, TiO_2 has been widely used in wastewater treatment for many years [14]. However, it suffers from some drawbacks. TiO_2 can easily form aggregates in a suspension resulting in a significant reduction in both its effective surface area and photocatalytic efficiency [15]. Before measuring the UV–Vis absorption, TiO_2 has to be separated by filtration or ultracentrifugation since it forms a finely dispersed

suspension in dye solution [16]. These challenges should be properly addressed for making more efficient utilization of TiO_2 in wastewater treatment.

Although the isolation of TiO_2 nanoparticles from solution is difficult, the immobilization of TiO_2 on the surface of a suitable particulate substrate makes the separation process easier [17]. The natural structure of clay minerals offers significant technological advantages in terms of stability and photocatalytic activity when TiO_2 is immobilized on the surface of clay [18,19]. Most of the self-synthesized TiO_2 is highly photoactive in its anatase form and the formation of Ti–O–Si bonds between TiO_2 and kaolinite prevents the phase transformation from the anatase to rutile phase [20]. Another issue with TiO_2 is that it has a higher electron–hole pair recombination rate, which results in lower photocatalytic activity within a short period of time [21]. This issue can be alleviated by doping TiO_2 with some other metal oxides like ZnO or Al_2O_3. ZnO is preferable since it has energy band structures and physical properties similar to TiO_2 [21]. The chemical combination of ZnO with TiO_2 leads to the reduction in recombination loss in TiO_2 due to comparatively better electronic mobility in ZnO [22]. A few binary composite photocatalysts having TiO_2/kaolinite and TiO_2/ZnO have been reported in the literature [18–24]. However, to the best of our knowledge, the synergistic impact of kaolinite, TiO_2 and ZnO towards the photocatalytic degradation of textile dyes has not been reported anywhere. Here, we report an effective thermochemical approach for developing a novel ternary composite photocatalyst from kaolinite, TiO_2 and ZnO. The ternary composite, $K_{0.50}T_{0.45}Z_{0.05}$, displayed 98% photocatalytic degradation of Remazol Red (RR) at 25°C within 2 h. Therefore, we highly expect that this novel photocatalyst will draw tremendous attention from researchers in academia and industry for efficient wastewater treatment.

2. Experimental

2.1 *Materials*

Commercial TiO_2 and ZnO were purchased from Merck KGaA (64271 Darmstadt, Germany). For the fabrication of a ternary photocatalyst, locally available kaolinite was utilized together with TiO_2 and ZnO. The model azo dye, RR, was collected from a local textile industry in Bangladesh. For adjusting the pH of dye solution, 35% (w/w) HCl acid and NaOH pellets were collected from Active Fine Chemicals Limited (Dhaka, Bangladesh). All the chemicals were used without further purification.

2.2 *Methods*

2.2a *Preparation of photocatalyst*: The precursors of ternary photocatalysts i.e., kaolinite, TiO_2 and ZnO were mixed in different proportions in deionized water. For homogeneous dispersion of the precursors, the mixture was sonicated at 50°C for 1 h. The solid mass, after being isolated from the water phase, was dried in an oven at 100°C for 1 h. The completely dried product was ground into fine powder prior to calcination at different temperatures in a muffle furnace. The high-temperature calcination created the suitable thermochemical environment for the synthesis of the composite. The composites were powdered again before performing a photocatalytic degradation study.

2.2b *Characterization of photocatalyst*: The chemical interaction was well understood *via* recording spectra on an FT-IR 8400S spectrometer (Shimadzu Corporation, Japan) operating in the wavenumber range of 4000–400 cm^{-1}. X-ray diffraction (XRD) patterns of the samples were recorded on an X-ray diffractometer (Ultima IV, Rigaku Corporation, Japan) at room temperature. CuKα radiation ($\lambda = 0.154$ nm), from a broad focus Cu tube operating at 40 kV and 40 mA, was applied to the samples. The XRD patterns were recorded in the continuous scanning mode with a scan speed of 3° min^{-1} and in the scan range of 10–70°. The thermal stability of the samples was investigated by recording thermograms on a thermogravimetric analyser (TGA-50, Shimadzu Corporation, Japan). The variation in morphological features was investigated by using an analytical scanning electron microscope (SEM) (JEOL JSM-6490LA, Tokyo, Japan) operating at an accelerating voltage of 20 kV. In order to find the elemental composition in the ternary composite, field emission scanning electron microscopy (FE-SEM) (JEOL JSM 7600F, Japan) fitted with an energy dispersive X-ray (EDX) analyser was employed.

2.2c *Photocatalytic degradation study*: The photocatalytic experiments were carried out under similar conditions of sunny days between BST (Bangladesh Standard Time) 11:15 am and 1:15 pm. The concentration of RR before and after degradation was measured by taking absorbance at 518 nm from a UV–Vis spectrophotometer (UV-2100PC Human Lab Instrument Co., Korea). Irradiation was carried out under open-air conditions with a 100 ml borosilicate glass beaker. The photocatalytic degradation of RR was performed at various conditions of operating time, pH and concentration. The degradation was monitored within 15 min time interval and percentage degradation was calculated from the absorbance data.

3. Results and discussion

3.1 *Characterization of ternary composite*

The chemical interaction among three components was well understood from the Fourier transform infrared (FTIR) spectra as depicted in figure 1a. The characteristic absorption bands of kaolinite at 1115 and 1004 cm^{-1} were submerged leading to a single peak at 1035 cm^{-1} in the ternary composite. Additionally, the two other characteristic peaks of kaolinite

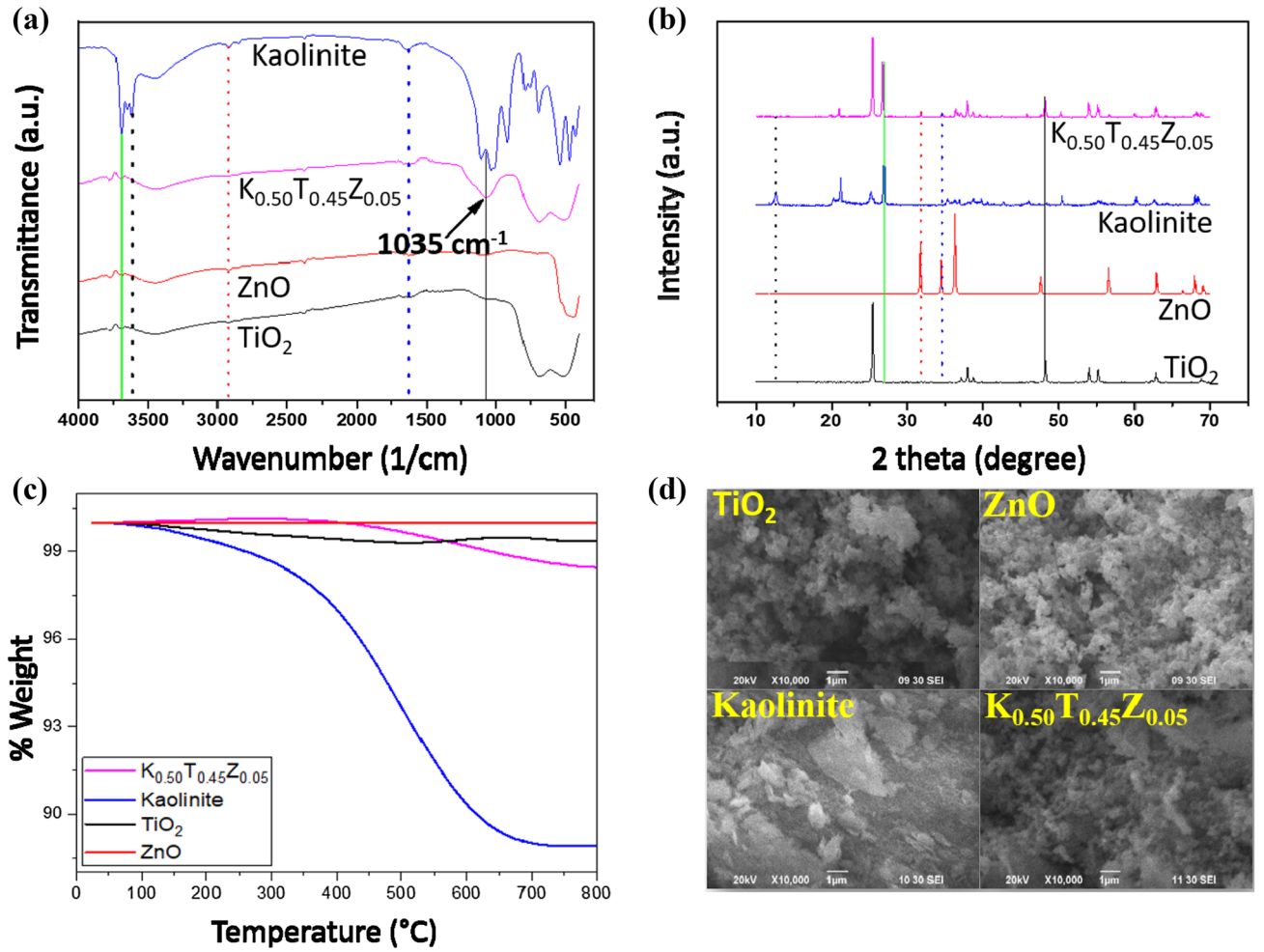

Figure 1. (**a**) FTIR spectra of kaolinite, TiO_2, ZnO and $K_{0.50}T_{0.45}Z_{0.05}$. The characteristic absorption bands of kaolinite at 1115 and 1004 cm^{-1} were submerged leading to a single peak at 1035 cm^{-1} in the ternary composite. (**b**) XRD patterns of the samples. The crystalline geometry of the ternary composite was different from the starting components. (**c**) TGA thermograms of the samples. The ternary composite showed a reduced mass loss at 800°C compared to kaolinite. (**d**) SEM microphotographs of the samples at ×10,000 magnifications. Both TiO_2 and ZnO displayed similar morphological features, however, the morphology of $K_{0.50}T_{0.45}Z_{0.05}$ was greatly controlled by the kaolinite content. The comparison in this figure strongly supports that high-temperature calcination brought significant chemical, structural, thermal and morphological variation in the ternary composite.

at 3640 cm^{-1} (O–H stretching) and 3670 cm^{-1} (Al–O–H stretching) completely disappeared in the ternary composite due to high-temperature calcination [25]. The variation in crystalline geometry is clearly illustrated and compared in figure 1b. As demonstrated in the XRD patterns, the characteristic peaks of the starting components are clearly present in the ternary composite with varying intensities depending on their relative contribution in terms of composition. The starting kaolinite showed a well-defined reflection at 2θ around 12.4°, which is a characteristic reflection from the [001] plane [25]. However, as indicated by the black dotted line, this peak completely disappeared in the ternary composite as the catalyst was synthesized *via* calcination at high temperature. From this figure, it is also evident that apart from chemical interactions, the starting components underwent significant structural rearrangements during the formation of the ternary composite. Thermogravimetric analysis (TGA) was carried out to investigate the thermal stability of the fabricated ternary composite. As shown in figure 1c, both TiO_2 and ZnO were thermally stable and showed a negligible mass loss even at 800°C. However, the starting kaolinite showed 11% mass loss at 800°C. It is interesting to note that the ternary composite fabricated from 50% kaolinite displayed only 1.5% mass loss at 800°C. From the TGA, it can be said that high-temperature calcination assisted kaolinite to combine chemically with both TiO_2 and ZnO. The thermal stability of kaolinite was dramatically improved after calcination due to the chemical interaction with highly stable TiO_2 and ZnO. Figure 1d compares the morphological features of kaolinite, TiO_2 and ZnO with those of the ternary composite.

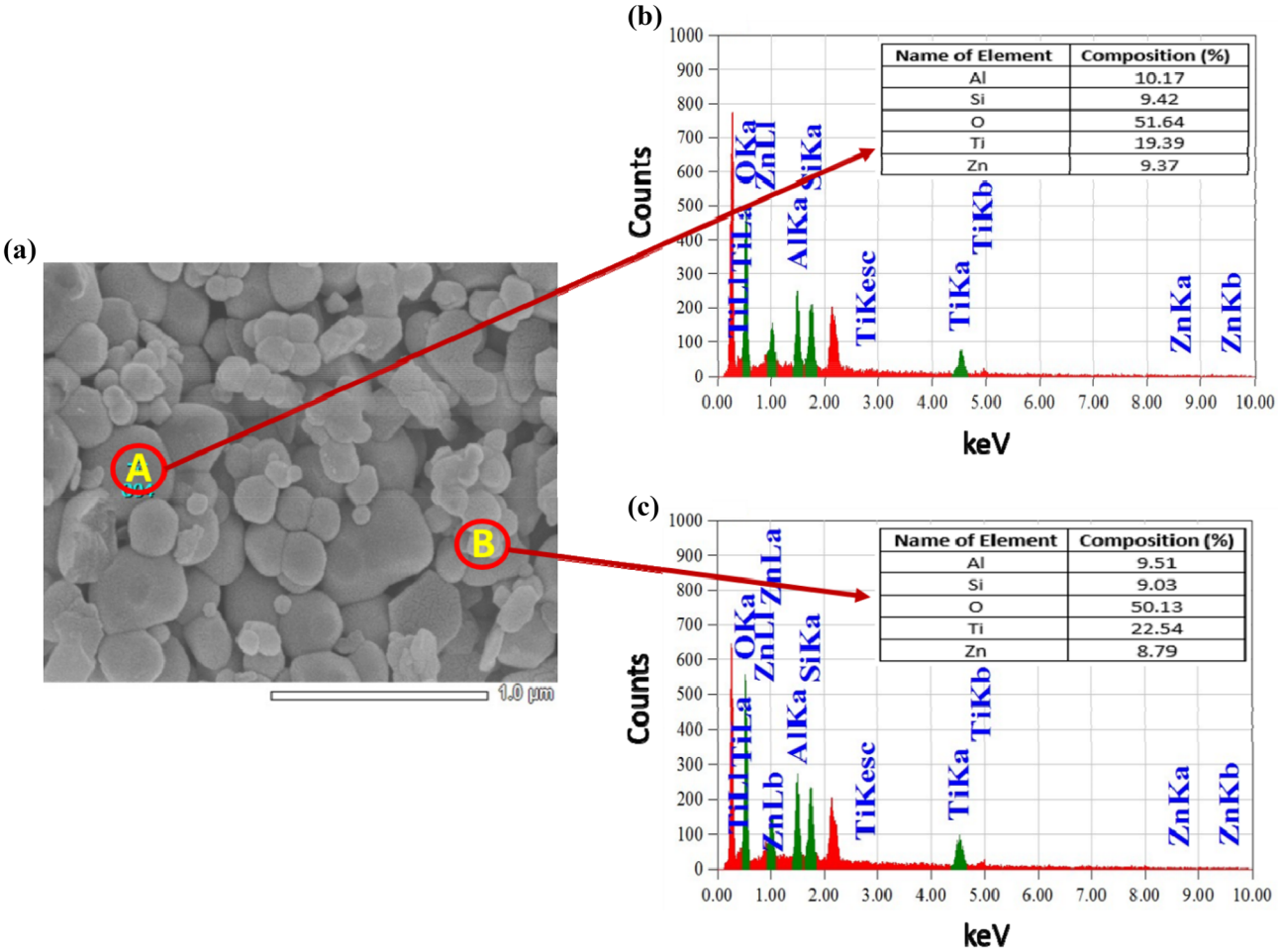

Figure 2. (**a**) FE-SEM image of $K_{0.50}T_{0.45}Z_{0.05}$ at ×50,000 magnifications. Variation in the size and shape of the particles is clearly understood from the FE-SEM image. (**b**, **c**) EDX spectra of $K_{0.50}T_{0.45}Z_{0.05}$ at two different positions A and B. Insets in figure 2b and c indicate the corresponding elemental composition at points A and B. EDX analysis confirmed the nearly homogeneous distribution of five elements (Al, Si, O, Ti and Zn).

It is evident that both TiO_2 and ZnO displayed similarity in the morphology with a homogeneous surface structure. On the other hand, the morphology of kaolinite was completely different from that of TiO_2 and ZnO. Kaolinite was rather found in the agglomerated state having non-homogeneous distribution of particles. High-temperature calcination brought significant variation in the morphology of the ternary composite by chemically combining TiO_2 and ZnO with kaolinite. The morphological feature of $K_{0.50}T_{0.45}Z_{0.05}$ is more clearly understood from the FE-SEM image shown in figure 2a. The distribution of both regularly and irregularly shaped particles was identified in the FE-SEM image of $K_{0.50}T_{0.45}Z_{0.05}$. The particle size of $K_{0.50}T_{0.45}Z_{0.05}$ was found to be in the range of 60–500 nm. As depicted in figure 2b and c, EDX analysis at two different particles confirmed the nearly homogeneous distribution of corresponding elements (Al, Si, O, Ti and Zn) in the ternary composite. The variation of elemental composition at two different positions might be attributed to the uncertainty involved with the EDX analysis. However, the elemental composition was close to the calculated composition based on the relative percentage of the three starting components. Since oxygen was predominantly present in all the starting components (kaolinite, TiO_2 and ZnO), more than 50% oxygen was quantified in the EDX analysis of the ternary composite. Similarly, the elemental composition of Al, Si, Ti and Zn was in well agreement corresponding to the relative proportion of kaolinite, TiO_2 and ZnO used for the fabrication of $K_{0.50}T_{0.45}Z_{0.05}$. The analytical techniques used in this study including FTIR, XRD, TGA, SEM and EDX strongly support that the high-temperature chemical interaction among the three components resulted in the successful fabrication of a ternary composite.

3.2 *Degradation of RR by ternary catalyst*

3.2a *Effect of calcination temperature*: Calcination temperature plays a potential role in synthesizing the composite photocatalyst. According to figure 3a, the ternary photocatalyst was effective when synthesized within the temperature range of 200–600°C. However, almost complete degradation

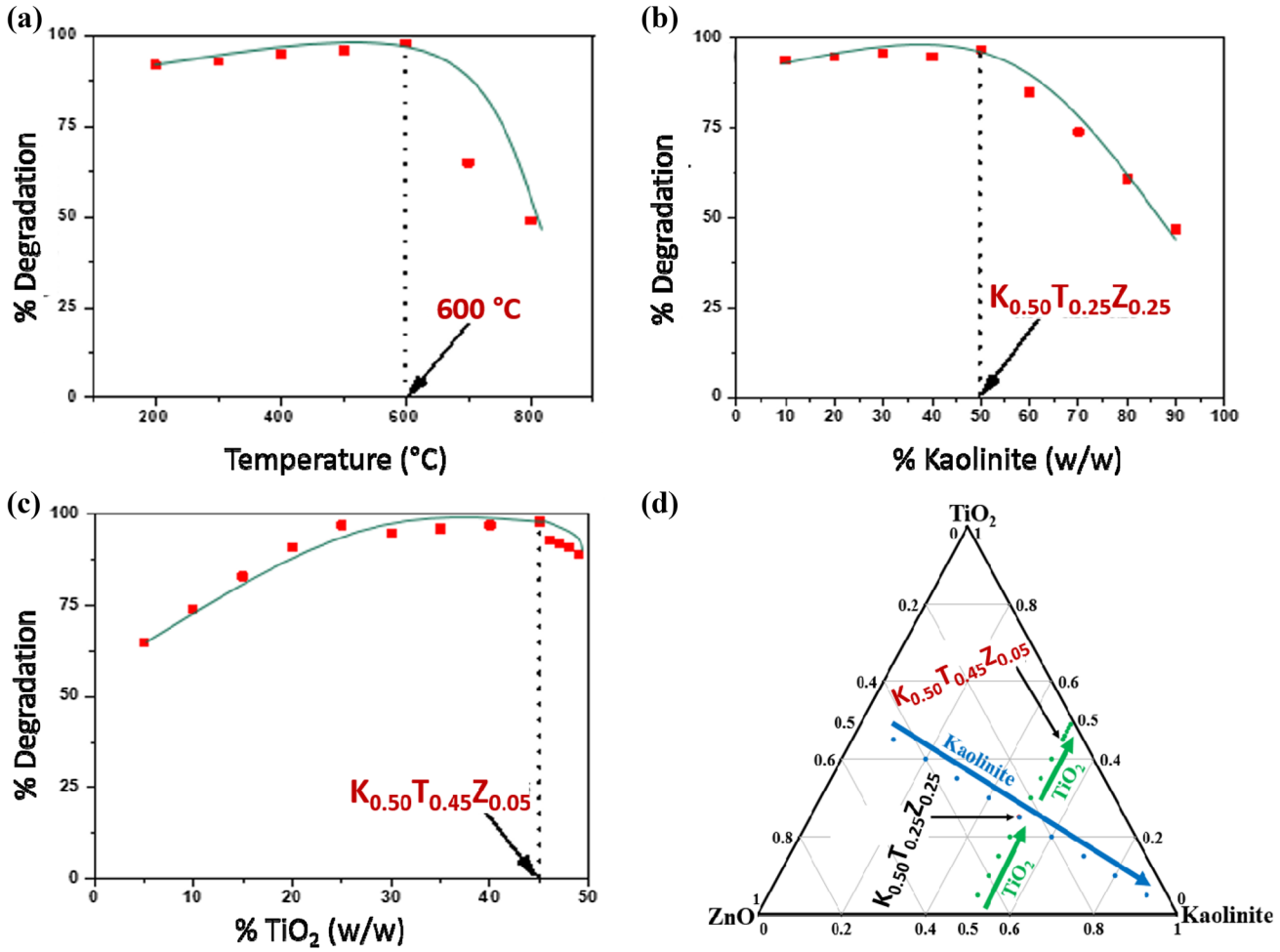

Figure 3. (**a**) Effect of calcination temperature on the photocatalytic performance of the composites. The maximum degradation of RR was recorded with the catalyst synthesized at 600°C. The effect of (**b**) kaolinite and (**c**) TiO_2 contents on the degradation of RR. (**d**) Representation of the relative contribution from three starting components in the degradation of RR in a simplified ternary diagram. It is clearly understood that the kaolinite content dramatically controlled the magnitude of degradation and the highest photocatalytic degradation was found with the ternary composite synthesized from 50% kaolinite (w/w), 45% TiO_2 and 5% ZnO (w/w) i.e., $K_{0.50}T_{0.45}Z_{0.05}$.

of RR was found when the catalyst was formed at 600°C. At temperature above 600°C, the degradation decreased sharply since kaolinite starts to lose its structural hydroxyl groups around this temperature [26]. Consequently, kaolinite failed to contribute to the synergistic impact that previously resulted in favourable catalyst dye interactions. As a result, degradation was severely paralysed above this temperature. The transformation of TiO_2 from the anatase to rutile phase was also responsible for the lower degradation of RR after 650°C [27].

3.2b *Effect of compositional variation*: In order to identify the most effective composite out of numerous possible compositions, a logical and sequential approach was taken. Since it was the major intention to maximize the contribution from kaolinite in the ternary photocatalyst, we started with 10% kaolinite (w/w) and proceeded with a gradual increase in the kaolinite content by keeping TiO_2 and ZnO contents in equal proportion. As illustrated in figure 3b, the maximum degradation of RR was found with the catalyst synthesized from 50% kaolinite (w/w), 25% TiO_2 (w/w) and 25% ZnO (w/w) i.e., $K_{0.50}T_{0.25}Z_{0.25}$. From this observation, we concluded that a maximum amount of 50% kaolinite (w/w) could be successfully loaded into the ternary catalyst system. Afterwards, the binary composition of TiO_2 and ZnO was varied by keeping the kaolinite content fixed at 50% (w/w). Finally, $K_{0.50}T_{0.45}Z_{0.05}$ was found to be the most effective ternary catalyst with 98% degradation of RR, which has been clearly demonstrated in figure 3c. Here, it can easily be predicted that at this critical composition, the surface chemical interaction, molecular architecture of the ternary catalyst and its morphological features created the most suitable aqueous environment for the effective interaction with the dye molecules. For better understanding of the relative

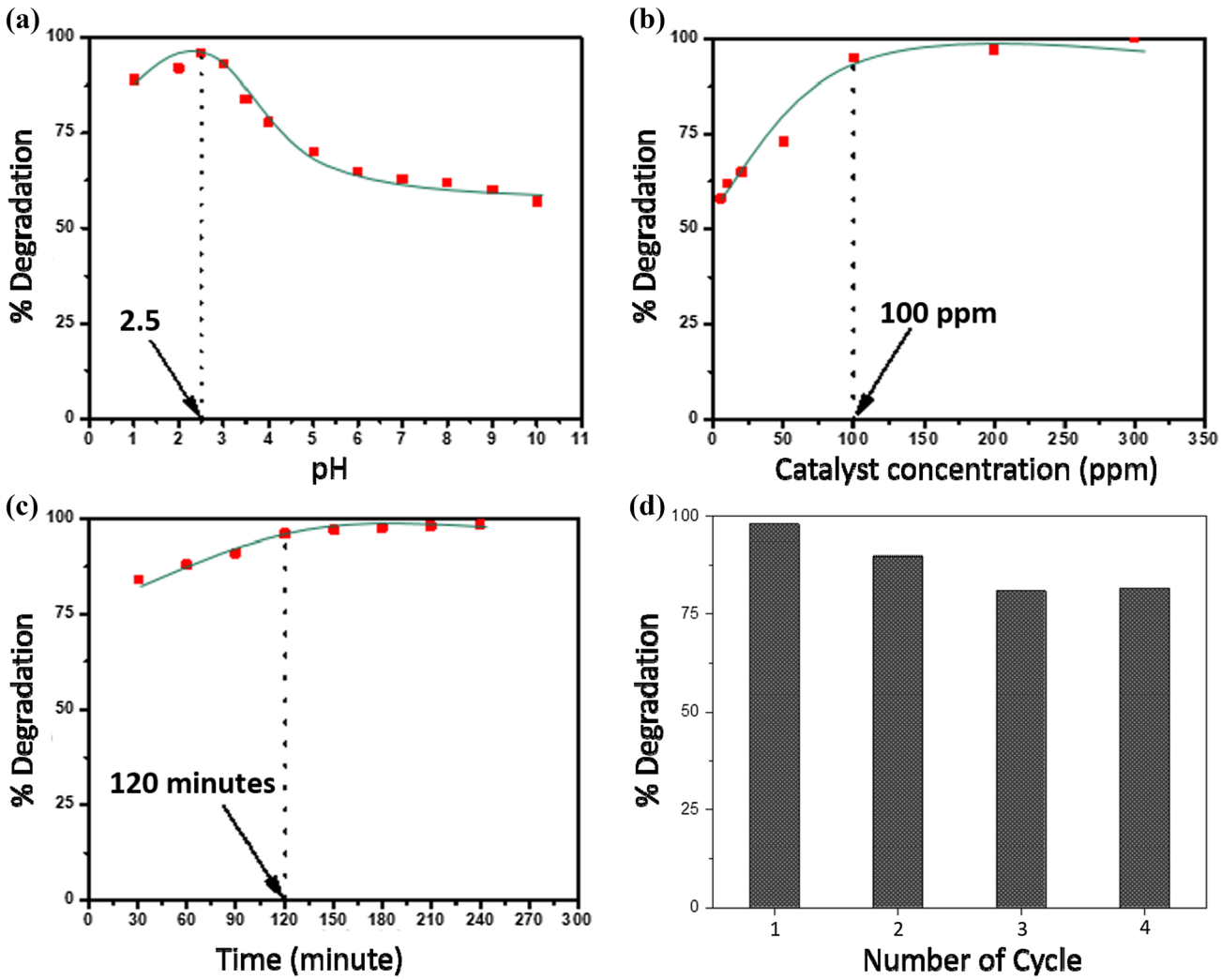

Figure 4. (**a**) Effect of pH on the degradation of RR. The positively charged catalyst surface was responsible for the degradation of RR and the maximum photocatalytic degradation was recorded at pH 2.5. The effect of (**b**) catalyst concentration and (**c**) time on the degradation of RR. The rate of degradation was found to increase with increasing catalyst concentration and operating time. However, the photocatalytic process reached equilibrium with 100 ppm catalyst after 120 min. (**d**) Bar chart representing the recyclability of the ternary composite. The chart indicates that the catalyst was suitable for long-term repeated applications.

contribution to the photocatalytic performance from the three starting components, a ternary diagram has been developed, which is displayed in figure 3d.

3.2c *Effect of pH*: The degradation of RR was found to be maximum at pH 2.5 (figure 4a). At this pH, the protonated catalyst surface might strongly attract negatively charged dye molecules, which ultimately resulted in subsequent photocatalytic degradation. It is reported in the literature that the photocatalytic activity is higher at lower pH, however, the presence of an excess amount of H^+ in the solution causes a decrease in degradation [28]. At pH lower than 2.5, probably the interaction of protons with azo linkage caused a decrease in electron density at the azo group resulting in lower photocatalytic degradation. However, as the pH was increased further, the degradation of anionic RR decreased gradually. At a higher pH value, there was less number of protons and as a result, there were superfluous negative charges, which led to the repulsion with anionic RR [29]. This phenomenon resulted in a decrease in degradation.

3.2d *Effect of catalyst concentration*: As displayed in figure 4b, it is seen that the degradation of RR increased gradually with an increase in the catalyst concentration up to 100 ppm. This phenomenon occurred probably due to the increased number of active sites with an increase in the catalyst concentration. It is also understood from the figure that there was only 2% increase in degradation when the catalyst concentration was changed from 100 to 200 ppm. Thus, extending beyond 100 ppm catalyst loading is not economically feasible as it did not increase the degradation

significantly. Hence, 100 ppm catalyst loading was taken as the optimum for further study.

3.2e *Effect of contact time*: From figure 4c, we can see that the percent degradation increased with an increase in irradiation time. This occurred because with more time more dyes got adsorbed at the catalyst surface and as a result more dyes were degraded. The generation of radicals was higher with the passage of time, which resulted in an increased degradation rate. However, after irradiation time of 120 min, the reaction rate reached equilibrium. This occurred because of the competition between the reactants and the intermediate products formed during degradation [30]. The slow degradation after 120 min was due to the slow reaction of radicals and photocatalysts because of the active site deactivation by strong by-product deposition [30].

The photocatalytic performance of the ternary catalyst was compared with those of kaolinite, TiO_2, ZnO and other binary composites. However, the best catalytic performance was found with $K_{0.50}T_{0.45}Z_{0.05}$ (table 1). From this comparison, we came to a conclusion that the synergistic impact in the ternary composite was comparatively better than those of binary composites and individual components. Besides, 50% loading of inexpensive kaolinite in the novel composite was undoubtedly a milestone in photocatalyst research.

Table 1. Performance comparison of various photocatalysts.

Catalyst system	% Degradation
Kaolinite	Nil
TiO_2	85
ZnO	82
$K_{0.50}T_{0.50}$	87
$K_{0.50}Z_{0.50}$	84
$T_{0.50}Z_{0.50}$	88
$K_{0.50}T_{0.45}Z_{0.05}$	98

3.3 *Control experiments*

In the control experiment without any catalyst, the RR concentration remained unchanged even after 120 min of irradiation. This result indicated that RR did not undergo photolysis under the applied conditions. Another experiment was carried out in the dark to understand the effect of sunlight on the degradation of RR. Only 6% degradation of RR was recorded in the dark after 120 min, which might occur due to the adsorption of dye molecules on the catalyst surface. From the blank experiments, it was concluded that photodegradation of RR was impossible without the synergistic contribution from both catalyst and solar irradiation.

3.4 *Reusability of the ternary catalyst*

The reusability of a photocatalyst is very crucial for its industrial application. Deactivation of the catalyst is a frequently encountered phenomenon due to its chemical interaction with various radicals. Therefore, to regenerate a catalyst it is expected to be recycled by simple treatment after the experiment. In this study, the ternary catalyst was regenerated up to four cycles. After the degradation of RR, $K_{0.50}T_{0.45}Z_{0.05}$ was recovered from the aqueous phase *via* centrifugation and was washed properly with copious deionized water.

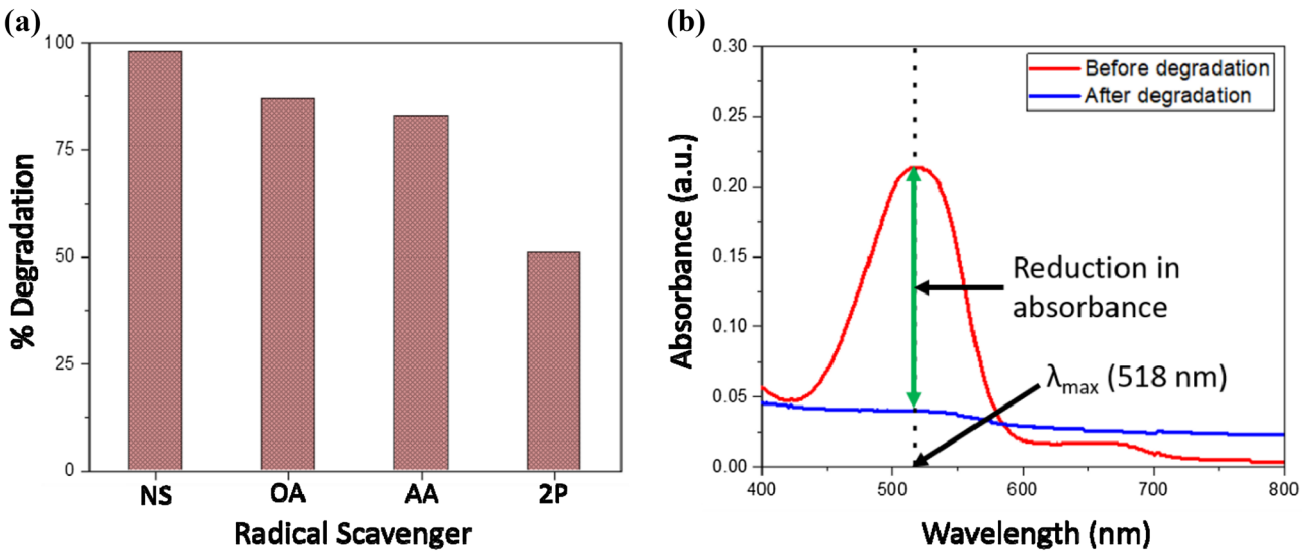

Figure 5. (**a**) Bar diagram representing the results of radical trapping experiments. The mechanistic investigation supported that photocatalytic degradation was mainly governed by hydroxyl radicals, while hole and superoxide radicals played only a minor role in the degradation of RR. (**b**) Visible spectra of dye solution before and after degradation. The reduction in absorbance at 518 nm confirmed that the developed ternary catalyst was highly efficient in completely degrading the dye under solar irradiation.

The dried mass was reused in the successive photodegradation experiments. The results from these experiments are clearly displayed in figure 4d. The bar chart indicates that the performance of the catalyst was satisfactory even in the fourth cycle i.e., the catalytic performance was not paralysed due to successive applications. However, the gradual decrease in the photocatalytic performance with the number of repeated uses might result from the poisoning effect of degraded products on the active sites of the catalyst, which could block the solar radiation to reach the catalyst surface. From this experiment it can be said that the ternary catalyst is suitable for long-term repeated use for degradation of toxic organic pollutants in the environment.

3.5 *Mechanistic details of the photocatalytic process*

In order to investigate the insights into the degradation mechanism, radical trapping experiments were carried out to identify the potential contribution from various active species towards the degradation of the dye molecules. In this experiment, oxalic acid (OA) was introduced as the hole scavenger [31], ascorbic acid (AA) as the superoxide radical scavenger [32] and 2-propanol (2P) as the hydroxyl radical scavenger [33]. These three particular quenchers were selected based on the fact that for degrading organic pollutants, hole, superoxide and hydroxyl radicals play a vital role under visible light irradiation [34]. For comparison purpose, another experiment was performed with no scavenger (NS). The results of the radical trapping experiments are shown in figure 5a. As shown in the figure, 98% degradation of RR was found in the absence of any scavenger, while 87% degradation was found with OA and 83% with AA, respectively. This finding indicates that both hole and superoxide radicals played only a minor role in the degradation process. However, the potential quenching effect was observed in the presence of 2P. Due to the introduction of 2P, degradation of RR was potentially reduced to 51%. From this trapping experiment, it can be concluded that the hydroxyl radical was mainly responsible for the photocatalytic degradation of RR. For further confirmation of nearly complete degradation, the visible spectrum of the degraded solution was recorded (figure 5b). The drastic reduction of absorbance at 518 nm (λ_{max}) strongly supports that the developed ternary catalyst was capable of nearly complete degradation of RR solution at pH 2.5 within 2 h of irradiation.

4. Conclusion

In this study, an effective ternary photocatalyst was successfully synthesized *via* calcination at 600°C. To the best of our knowledge, a ternary photocatalyst from kaolinite, TiO_2 and ZnO has not been reported before. However, the major success of this study was the loading of 50% kaolinite (w/w) in the catalyst, which made the synthesis of the catalyst a less expensive. The challenges that are usually encountered when using TiO_2 as a catalyst alone were successfully resolved by the synergistic contribution from kaolinite and ZnO. Besides, the immobilization of TiO_2 on the large available surface of stable kaolinite significantly improved the photocatalytic performance of TiO_2. To sum up, it is quite evident that the photocatalytic efficiency of $K_{0.50}T_{0.45}Z_{0.05}$ together with its cost-effective nature has made it a promising candidate for the effective treatment of effluents from various industries including textile, food, leather, pharmaceuticals, food, paint, etc.

Acknowledgements

The authors are grateful to the Centre for Advanced Research in Sciences (CARS), University of Dhaka, Bangladesh for providing partial analytical support. The authors also thank the Ministry of Science and Technology, Bangladesh, for providing financial support (Grant No. 39.00.0000.09.06.79. 2017/Es-57/285) to carry out this research.

References

[1] Kivaisi A K 2001 *Ecol. Eng.* **16** 545
[2] Abdel R W 2000 *Biomed. Environ. Sci.* **13** 219
[3] Chung K T 2016 *J. Environ. Sci. Health, Part C* **34** 233
[4] Wang Y T and Chirwa E M 1998 *Water Sci. Technol.* **38** 113
[5] Tziotzios G, Dermou E, Politi D and Vayenas D V 2008 *J. Chem. Technol. Biotechnol.* **83** 829
[6] Debadatta D and Susmita M 2012 *J. Environ. Res. Dev.* **7** 946
[7] Herrmann J M 1999 *Catal. Today* **53** 115
[8] Mozia S, Tomaszewska M, Kosowska B, Grzmil B, Morawski A W and Kałucki K 2005 *Appl. Catal. B: Environ.* **55** 195
[9] Lachheb H, Puzenat E, Houas A, Ksibi M, Elaloui E, Guillard C *et al* 2002 *Appl. Catal. B: Environ.* **39** 75
[10] Belhouchet N, Hamdi B, Chenchouni H and Bessekhouad Y 2019 *J. Photochem. Photobiol. A* **372** 196
[11] Su Y, Zhao X, Bi Y and Han X 2019 *Clean Technol. Environ. Policy* **21** 367
[12] Babu S G, Karthik P, John M C, Lakhera S K, Ashokkumar M, Khim J *et al* 2019 *Ultrason. Sonochem.* **50** 218
[13] Ge J, Zhang Y, Heo Y-J and Park S-J 2019 *Catalysts* **9** 122
[14] Nagaveni K, Sivalingam G, Hegde M S and Madras G 2004 *Appl. Catal. B: Environ.* **48** 83
[15] Wang C, Xu B Q, Wang X and Zhao J 2005 *J. Solid State Chem.* **178** 3500
[16] Kagaya S, Shimizu K, Arai R and Hasegawa K 1999 *Water Res.* **33** 1753
[17] Faramarzpour M, Vossoughi M and Borghei M 2009 *Chem. Eng. J.* **146** 79
[18] Kutláková K M, Tokarský J, Kovář P, Vojtěšková S, Kovářová A, Smetana B *et al* 2011 *J. Hazard. Mater.* **188** 212
[19] Chong M N, Vimonses V, Lei S, Jin B, Chow C and Saint C 2009 *Microporous Mesoporous Mater.* **117** 233
[20] Vimonses V, Chong M N and Jin B 2010 *Microporous Mesoporous Mater.* **132** 201
[21] Famojuro A T, Ojo I A O, Egharevba G O and Maaza M A 2013 *Ife J. Sci.* **15** 321
[22] Habibi M H and Mikhak M 2012 *Appl. Surf. Sci.* **258** 6745

[23] Lopes J da S, Rodrigues W V, Oliveira V V, Braga A do N S B, Silva R T, França A A C *et al* 2019 *Appl. Clay Sci.* **168** 295
[24] Kubiak A, Siwińska-Ciesielczyk K, Bielan Z, Zielińska-Jurek A and Jesionowski T 2019 *Adsorption* **25** 309
[25] Saikia B J and Parthasarathy G 2010 *J. Mod. Phys.* **1** 206
[26] Kakali G, Perraki T H, Tsivilis S and Badogiannis E 2001 *Appl. Clay Sci.* **20** 73
[27] Lu C, Sun X, Peng J and Ma Y 2013 *J. Chem. Soc. Pak.* **35** 42
[28] Rauf M A and Ashraf S S 2009 *Chem. Eng. J.* **151** 10
[29] Sun J, Wang X, Sun J, Sun R, Sun S and Qiao L 2006 *J. Mol. Catal. A Chem.* **260** 241
[30] Konstantinou I K and Albanis T A 2004 *Appl. Catal. B: Environ.* **49** 1
[31] Adamu H, McCue A J, Taylor R S F, Manyar H G and Anderson J A 2019 *J. Environ. Chem. Eng.* **7** 103029
[32] Molla M A I, Tateishi I, Furukawa M, Katsumata H, Suzuki T and Kaneco S 2017 *Open J. Inorg. Non-Met. Mater.* **7** 1
[33] Venkatesh D, Pavalamalar S and Anbalagan K 2019 *J. Inorg. Organomet. Polym. Mater.* **29** 939
[34] Shi Y, Yang D, Li Y, Qu J and Yu Z-Z 2017 *Appl. Surf. Sci.* **426** 622